

Tagging sneutrino resonances at a linear collider with associated photons

Debajyoti Choudhury,^{1,*} Santosh Kumar Rai,^{2,†} and Sreerup Raychaudhuri^{2,‡}

¹*Department of Physics & Astrophysics, University of Delhi, Delhi 110 007, India*

²*Department of Physics, Indian Institute of Technology, Kanpur 208 016, India*

(Received 29 January 2005; published 16 May 2005)

Sneutrino resonances at a high-energy linear e^+e^- collider may be one of the clearest signals of supersymmetry without R parity, especially when the R -parity-violating coupling is too small to produce observable excesses in four-fermion processes. However, there is no guarantee that the sneutrino pole will lie anywhere near the machine energy. We show that associated photon production induces the necessary energy spread, and that the resonance then leaves a clear imprint in the photon spectrum. It follows that tagging of a hard monoenergetic photon for a variety of possible final states provides a realistic method of separating sneutrino resonance signals from the standard model backgrounds.

DOI: 10.1103/PhysRevD.71.095009

PACS numbers: 14.80.Ly, 12.60.Jv

I. INTRODUCTION

In many models of supersymmetry, R parity [1,2], defined as $R_p = (-)^{L+3B+2S}$, where L , B and S stand, respectively, for the lepton number, baryon number, and spin of a particle, is often assumed to be conserved. A conservation law of this kind is clearly tantamount to separate conservation¹ of both the global $U(1)$ quantum numbers L and B . This idea, originally introduced to combat fast proton decay, has since been shown to be necessary only in part. It is enough to conserve either lepton number L or baryon number B —and not both—to have the requisite stability for protons. Furthermore, there does not exist any other overriding theoretical motivation for imposing this symmetry. In fact, it has been argued [3] that stability of the proton is better ensured by imposing a generalized baryon parity (a Z_3 symmetry) instead. Unlike R parity, the latter also serves to eliminate dimension-5 operators that could potentially have led to proton decay. This has the added advantage that nonzero \mathcal{K}_p couplings provide a means of generating the small neutrino masses and large mixings that the neutrino oscillation experiments seem to call for.

In this paper, we assume that baryon number is conserved and concentrate on R -parity violation through lepton number-violating operators of the so-called $LL\bar{E}$ form. The relevant term in the superpotential can be written as

$$\mathcal{W}_{LL\bar{E}} = \lambda_{ijk} \epsilon_{ab} \hat{L}_i^a \hat{L}_j^b \hat{E}_k, \quad i, j = 1 \dots 3, \quad (1)$$

where $\hat{L}_i \equiv (\hat{\nu}_{Li}, \hat{\ell}_{Li})^T$ and \hat{E}_i are the $SU(2)$ -doublet and singlet superfields, respectively, whereas ϵ_{ab} is the unit antisymmetric tensor. Clearly, the coupling constants λ_{ijk} are antisymmetric under the exchange of the first two indices; the 9 such independent couplings are usually labeled keeping $i > j$. In the above it is assumed that the chiral structure of the standard model (SM) holds and any

interaction terms with right-handed neutrinos (or corresponding superfields) would be strongly suppressed by the tiny neutrino masses. Written in terms of the component fields, the above superpotential leads to the interaction Lagrangian

$$\begin{aligned} \mathcal{L}_\lambda = & \lambda_{ijk} [\tilde{\nu}^i \bar{\ell}_R^k \ell_L^j + \tilde{\ell}_L^j \bar{\ell}_R^k \nu_L^i + (\tilde{\ell}_R^k)^* \overline{(\nu_L^i)^c} \ell_L^j \\ & + (\tilde{\nu}^i)^* \bar{\ell}_L^j \ell_R^k + (\tilde{\ell}_L^j)^* \bar{\nu}_L^i \ell_L^k + \tilde{\ell}_R^k \bar{\ell}_L^j (\nu_L^i)^c - \tilde{\nu}^i \bar{\ell}_R^k \ell_L^i \\ & - \tilde{\ell}_L^i \bar{\ell}_R^k \nu_L^j - (\tilde{\ell}_R^k)^* \overline{(\nu_L^j)^c} \ell_L^i - (\tilde{\nu}^j)^* \bar{\ell}_L^i \ell_R^k \\ & - (\tilde{\ell}_L^i)^* \bar{\nu}_L^j \ell_L^k - \tilde{\ell}_R^k \bar{\ell}_L^i (\nu_L^j)^c]. \end{aligned} \quad (2)$$

Just like the usual Yukawa couplings, the magnitude of the couplings λ_{ijk} are entirely arbitrary, and are restricted only from phenomenological considerations. The preservation of a GUT-generated $B - L$ asymmetry, for example, necessitates the preservation of at least one of the individual lepton numbers over cosmological time scales [4]. Similarly, the failure of various collider experiments [5,6] to find any evidence of supersymmetry has implied constraints in the parameter space. Even if superpartners were too heavy to be produced directly, strong bounds on these couplings may still be deduced from the remarkable agreement between low energy observables and the SM predictions. These include, for example, meson decay widths [7,8], neutrino masses [8,9], rates for neutrinoless double beta decay [10], etc. The bounds generally scale with the sfermion mass and, for $m_{\tilde{f}} = 100$ GeV, they range from ~ 0.02 to 0.8 [11]. In view of such constraints, strategies for collider signals for R_p -violating supersymmetry are often designed for scenarios wherein the production of the superparticles is dominated by gauge couplings and the leading role of R_p violation is in the decay of the lightest supersymmetric particle (LSP) [12]. Clearly, such studies would be insensitive to the exact size of the R_p -violating coupling as long as it is large enough to make the decay length of the LSP undetectable². In con-

*Electronic address: debchou@physics.du.ac.in

†Electronic address: skrai@iitk.ac.in

‡Electronic address: sreerup@iitk.ac.in

¹Strictly speaking, this is true only if we restrict ourselves to renormalizable superpotentials.

²If any of the R_p -violating couplings is $> 10^{-6}$ or so, then the LSP will decay within the detector [13].

trast to this, processes directly sensitive to the size of such couplings would include (i) production of sparticles through them [14–16], (ii) the decays of sparticles through them [17,18] and (iii) modification of SM amplitudes through exchanges of virtual sparticles [15,17,19–23]. An accurate measurement of such cross sections can, apart from leading to the discovery of supersymmetry, also serve as a means of measuring the size of such couplings. In this paper, we concentrate on one such example, namely, single sneutrino production in association with a hard photon.

As we shall see presently, the terms relevant for our discussion are the first and fourth ones on both first and second lines of Eq. (2), with $j = k = 1$ on the first line and $i = k = 1$ on the second. Isolating these leads to the specific interactions

$$\begin{aligned} \mathcal{L}_\lambda &= -2\lambda_{1j1}[\tilde{\nu}^j \bar{e}_R e_L + (\tilde{\nu}_L^j)^* \bar{e}_L e_R] + \dots \\ &= -2\lambda_{121}[\tilde{\nu}_\mu \bar{e}_R e_L + (\tilde{\nu}_\mu)^* \bar{e}_L e_R] \\ &\quad - 2\lambda_{131}[\tilde{\nu}_\tau \bar{e}_R e_L + (\tilde{\nu}_\tau)^* \bar{e}_L e_R] + \dots, \end{aligned} \quad (3)$$

where the dots stand for the terms in Eq. (2) that are irrelevant to the present discussion. It is then a simple matter to read off the Feynman rules for the vertices

$$e^+ e^- \tilde{\nu}_\mu, \quad e^+ e^- \tilde{\nu}_\mu^*, \quad e^+ e^- \tilde{\nu}_\tau, \quad e^+ e^- \tilde{\nu}_\tau^*.$$

The presence of these vertices clearly leads to resonances in the processes [24]

$$\begin{aligned} e^+ + e^- &\rightarrow \tilde{\nu}_{\mu/\tau}(\tilde{\nu}_{\mu/\tau}^*) \rightarrow e^+ + e^- \rightarrow \tilde{\nu}_{\mu/\tau}(\tilde{\nu}_{\mu/\tau}^*) \\ &\rightarrow \nu_{\mu/\tau}(\bar{\nu}_{\mu/\tau}) + \tilde{\chi}_{1/2/3/4}^0 \rightarrow \tilde{\nu}_{\mu/\tau}(\tilde{\nu}_{\mu/\tau}^*) \\ &\rightarrow \mu^\mp/\tau^\mp + \tilde{\chi}_{1/2}^\pm, \end{aligned}$$

the first of which resembles Bhabha scattering in QED or in the SM. As in Bhabha scattering, the sneutrino exchange can occur in both s and t channels. For the other two it is simply an s -channel sneutrino exchange. It is also implicit that only those processes among the above will occur which are kinematically allowed, i.e. if the higher neutralino and chargino states are heavier than the sneutrino, the corresponding process will occur off-shell, with strong propagator suppression of the corresponding cross sections.

The sneutrino decay width, which is a simple matter to compute, never rises above 3–4 GeV, which means that at a collider with several hundred GeVs of energy, we can apply the *narrow-width approximation* with impunity. In this work, therefore, we solely consider on-shell production of sneutrinos (of muonic or tauonic flavor). It is also worth mentioning that, in line with most of the literature on R -parity violation, we consider only one nonvanishing (or dominant) λ coupling, for the simultaneous presence of more than one \mathcal{R}_p coupling could potentially lead to flavor-changing neutral currents and hence is subject to rather stringent constraints [25]. Though apparently unnatural,

this is not more so than the pattern of Yukawa couplings in the SM.

The principal issue on which this work hinges is the fact that a high-energy $e^+ e^-$ collider is likely to run at just a single (or a few fixed) center-of-mass energies \sqrt{s} . Given our present lack of knowledge of sneutrino masses (or even of the existence of sneutrinos) it is highly unlikely that for these predetermined machine energies we can have $\sqrt{s} \approx m_{\tilde{\nu}}$. If, indeed, $m_{\tilde{\nu}} < \sqrt{s}$, then the cross section for $e^+ + e^- \rightarrow \tilde{\nu}_{\mu/\tau}(\tilde{\nu}_{\mu/\tau}^*)$ will be strongly propagator suppressed. However, if we consider the process $e^+ + e^- \rightarrow \gamma + \tilde{\nu}_{\mu/\tau}(\tilde{\nu}_{\mu/\tau}^*)$, then, for some of the events, the photon may carry off just enough energy for the remaining $e^+ e^-$ system to excite the sneutrino resonance. To borrow from a much-used terminology, we are essentially considering a “radiative return to the sneutrino.” A similar method of detecting massive graviton resonances has been discussed in Ref. [26]. With processes of interest being of the form

$$\begin{aligned} e^+ + e^- &\rightarrow \gamma + \tilde{\nu}_{\mu/\tau}(\tilde{\nu}_{\mu/\tau}^*) \rightarrow \gamma + e^+ + e^- \\ &\rightarrow \gamma + \tilde{\nu}_{\mu/\tau}(\tilde{\nu}_{\mu/\tau}^*) \\ &\rightarrow \gamma + \nu_{\mu/\tau}(\bar{\nu}_{\mu/\tau}) + \tilde{\chi}_{1/2/3/4}^0 \\ &\rightarrow \gamma + \tilde{\nu}_{\mu/\tau}(\tilde{\nu}_{\mu/\tau}^*) \rightarrow \gamma + \mu^\mp/\tau^\mp + \tilde{\chi}_{1/2}^\pm, \end{aligned} \quad (4)$$

the application of the narrow-width approximation ensures an almost monochromatic photon of energy

$$E_\gamma = \frac{s - m_{\tilde{\nu}}^2}{2\sqrt{s}}. \quad (5)$$

This, potentially, would stand out against the continuum spectrum arising from the standard model background. Since the sneutrino $\tilde{\nu}_{\mu/\tau}$ can have a variety of decay channels, we can simply tag on a hard isolated photon associated with any of these decay channels and look for a line spectrum superposed on the continuum background. This will lead, as our discussion will show, to clear signals of sneutrino production. Moreover, the R -parity-violating decays of the sneutrino will set up multilepton final states (with associated photons) which will have little or no standard model backgrounds worth considering. For such states a monoenergetic photon will clinch the issue of sneutrino production. Our work establishes, therefore, that at a linear collider, R -parity-violating supersymmetry may be detected early through an associated photon, perhaps even before the conventional supersymmetry searches have collected enough statistics.

It is worth noting that the usual signature for R -parity-violating supersymmetry at an $e^+ e^-$ collider is through four-fermion processes of the form (for $LL\bar{E}$ operators) $e^+ e^- \rightarrow e^+ e^-$, $e^+ e^- \rightarrow \mu^+ \mu^-$, and $e^+ e^- \rightarrow \tau^+ \tau^-$, where the principal contribution is through t -channel sneutrino exchange. A simple consideration of the excess (over the SM) cross section [15] leads to a discovery limit of

about $\lambda_{1j1} = 0.04$ for the lepton number-violating coupling responsible for the signal, for $m_{\tilde{\nu}} \lesssim 200$ GeV. Our work is, therefore, principally concerned with signals for R -parity violation when the coupling is $\lambda_{1j1} \lesssim 0.04$, but the sneutrino is light enough to be produced as a resonance in e^+e^- collisions at the machine energies of 500 GeV and 1 TeV. In fact, one major advantage of studying resonant sneutrinos is that the parameter space of the model can be explored almost up to $m_{\tilde{\nu}} = \sqrt{s}$, except for a small reduction due to kinematic cuts on the final states observed. By contrast, slepton or sneutrino pair production has the potential to explore only $m_{\tilde{\nu}} \leq \sqrt{s}/2$.

This paper is organized as follows. In the next two sections we discuss, successively, the production cross section and different decay channels of the two sneutrinos which are under investigation. Section IV is devoted to a discussion of backgrounds and possible strategies to isolate the signal. In Sec. V, we discuss how a sneutrino resonance could be distinguished from other possible new physics effects. And finally, Sec. VI contains our conclusions and some general comments.

II. SNEUTRINO PRODUCTION WITH ASSOCIATED PHOTONS

The specific reaction on which we focus in this paper is the associated photon process

$$e^+ + e^- \rightarrow \gamma + \tilde{\nu}_{\mu/\tau}(\tilde{\nu}_{\mu/\tau}^*)$$

illustrated in Fig. 1. The squared and spin-averaged matrix element for this is, then

$$|\overline{\mathcal{M}}|^2 = 8\pi\alpha\lambda_{1j1}^2 \frac{s^2 + \tilde{m}_j^4}{tu} \theta(s - \tilde{m}_j^2), \quad (6)$$

where \tilde{m}_j is the mass of the muonic ($j = 2$) or tauonic ($j = 3$) sneutrino. The cross sections for production of the sneutrino and its antiparticle are identical; if we do not distinguish between the signals for these, the effective cross section must be multiplied by a factor of 2. The collinear singularity in Eq. (6), so characteristic of mass-

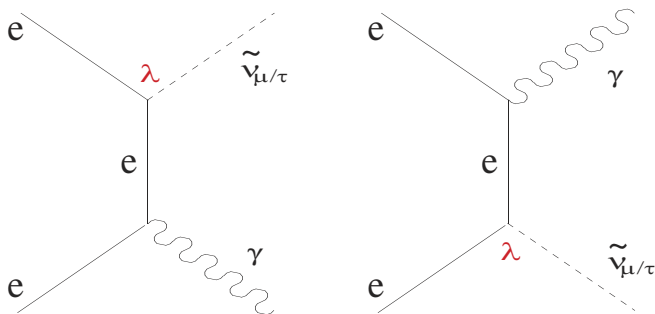


FIG. 1 (color online). Feynman diagrams for sneutrino production with associated photons at a linear collider.

less electrons and photons, is automatically taken care of once one imposes restrictions on the phase space commensurate with the detector acceptances. In the rest of the analysis, we shall require the photon to be sufficiently hard and transverse, namely

$$\begin{aligned} \text{pseudorapidity: } |\eta_\gamma| &< \eta_\gamma^{(\max)} = 2.0, \\ \text{transverse momentum: } p_{T\gamma} &> p_{T\gamma}^{(\min)} = 20 \text{ GeV}. \end{aligned} \quad (7)$$

Integrating Eq. (6) leads to a production cross section of the form

$$\begin{aligned} \sigma(x_j) &= \frac{2\alpha\lambda_{1j1}^2}{s} \frac{1+x_j^2}{1-x_j} \theta(1-x_j) \Omega_j, \\ \Omega_j &= \min \left[\eta_\gamma^{(\max)}, \log \frac{1-x_j - \sqrt{(1-x_j)^2 - 4x_T^2}}{2x_T} \right], \end{aligned} \quad (8)$$

where $x_j = \tilde{m}_j^2/s$ and $x_T = p_{T\gamma}^{(\min)}/\sqrt{s}$.

The cross section in Eq. (8) is plotted in Fig. 2 as a function of \tilde{m}_j and with $\lambda_{1j1} = 0.03$ for a linear collider running at (a) 500 GeV and (b) 1 TeV. Several comments are in order:

- (i) Contrary to naive expectations, the cross section rises

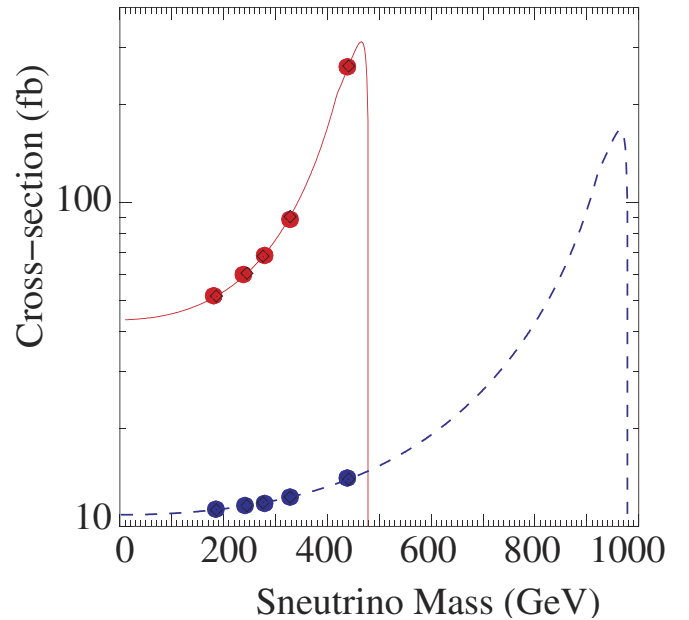


FIG. 2 (color online). Cross sections for sneutrino production with associated photons at a linear collider for $\lambda_{1j1} = 0.03$. Solid red (dashed blue) lines correspond to a 500 GeV (1 TeV) center-of-mass energy. The cuts of Eqs. (7) have been imposed. The points marked with bullets are for a $\tilde{\nu}_\mu$ resonance at the Snowmass MSugra points 1a, 1b, 3, 4, and 5. At the point 2, the sneutrino is beyond the kinematic reach of the linear collider. If sneutrinos are not distinguished from antisneutrinos, the cross section(s) would be doubled.

with the sneutrino mass (until nearly the kinematic limit). This is occasioned by the fact that a sneutrino mass closer to the center-of-mass energy implies that the photon needs to carry off less energy, thereby facilitating the radiative return to the sneutrino.

- (ii) A consequence of the above is the fact that, below the kinematic limit, the cross sections at a 500 GeV collider are larger than those at a 1 TeV machine.
- (iii) The steep fall in the cross section when the kinematic limit is approached occurs just a little before the actual threshold $m_{\tilde{\nu}} = \sqrt{s}/2$. This is simply a consequence of our having demanded a nonzero $(p_{T\gamma})^{(\min)}$.
- (iv) It is also interesting to note the very slight kink in the graph(s) a little before the falloff. This is another artifact of our cuts. Below this mass it is the restriction on η_γ that is mainly operative, while above this mass, it is the cut on $p_{T\gamma}$ that takes over. This is a discrete transition, causing the slight kink as

1a:	$M_0 = 100 \text{ GeV},$	$m_{1/2} = 250 \text{ GeV},$	$A_0 = -100 \text{ GeV},$	$\tan\beta = 10,$	$\mu > 0$
1b:	$M_0 = 200 \text{ GeV},$	$m_{1/2} = 400 \text{ GeV},$	$A_0 = 0,$	$\tan\beta = 30,$	$\mu > 0$
3:	$M_0 = 1450 \text{ GeV},$	$m_{1/2} = 300 \text{ GeV},$	$A_0 = 0,$	$\tan\beta = 10,$	$\mu > 0$
3:	$M_0 = 90 \text{ GeV},$	$m_{1/2} = 400 \text{ GeV},$	$A_0 = 0,$	$\tan\beta = 10,$	$\mu > 0$
4:	$M_0 = 400 \text{ GeV},$	$m_{1/2} = 300 \text{ GeV},$	$A_0 = 0,$	$\tan\beta = 50,$	$\mu > 0$
5:	$M_0 = 150 \text{ GeV},$	$m_{1/2} = 300 \text{ GeV},$	$A_0 = -1 \text{ TeV},$	$\tan\beta = 5,$	$\mu > 0$

At most of these Snowmass points, the muonic and taonic sneutrinos are almost degenerate (see Table I). In Fig. 2, five of the six mSugra points (1a, 1b, 3–5) have been marked with bullets (●). The Snowmass point numbered 2 leads to a sneutrino mass of 1.45 TeV which is clearly out of the kinematic range of a 500 GeV or even a 1 TeV linear collider. Note also that in each of these cases, the lightest neutralino is the lightest supersymmetric particle (LSP)³ This is quite clear from Table I, where we have listed the sneutrino masses and the masses of their daughters in possible decay channels.

The major hurdle in detection of sneutrinos will, of course, be isolation of the signal from the substantial standard model backgrounds, since massive sneutrinos can decay in a variety of channels, each with characteristic signatures. As there is a R -parity-violating λ coupling, we should expect several types of hadronically quiet multi-lepton signals. These are discussed in the section which follows.

³While this is a requirement for a R -parity conserving model to be phenomenologically viable, it clearly is not so in the event of a broken R parity.

mentioned.

- (v) As the graph shows, we obtain cross sections typically in the range 50–250 fb. At a linear collider with around 500 fb^{-1} of integrated luminosity, this amounts to the production of a very large number of sneutrinos along with an associated monochromatic photon. Thus, even if λ_{1j1} were to be smaller by an order of magnitude, we would still have a fairly large number of such distinctive events. It is clear, therefore, that if the sneutrino is kinematically accessible to a linear collider, low statistics will not be the major hurdle in their detection.

Although there is no strict restriction on the mass spectrum of R -parity-violating models (except for weak experimental bounds from LEP-2 and the Tevatron), it is useful, for the purpose of easy comparison, to focus on the MSugra spectrum and, specifically, on the six representative points chosen at the 2001 Snowmass conference. The latter are described by

III. DECAYS OF THE SNEUTRINO

Some of the sneutrino decays have already figured in the discussion of resonant processes. However, in R -parity-violating models, decays of the sneutrino are rather complex. Two distinct scenarios are identifiable though:

- (i) *Small- λ limit.*—When the R -parity-violating coupling λ_{1j1} is much smaller than the gauge couplings, the sneutrino decays principally through normal, R -parity-conserving, channels. In this case, R -parity violation manifests itself only in the decays of the neutralino LSP. Note, however, that unless $\lambda_{1j1} \lesssim 10^{-5}$ the LSP also decays almost at the interaction point into an invisible neutrino and a lepton pair (not necessarily of the same flavor). The final signal will, therefore, include the daughters of sneutrino decays as well as those arising from LSP decays. There are several such possibilities, depending on the mass spectrum, and hence each point in the parameter space has to be considered separately.
- (ii) *Large- λ limit.*—When the R -parity-violating coupling λ_{1j1} is comparable to the gauge couplings, the sneutrino will have a substantial decay width into an e^+e^- pair. In fact, this may even become the dominant decay mode.

TABLE I. Relevant parts of the MSugra spectrum for the six Snowmass points. All masses are in GeV, rounded off to the nearest whole number.

Point	$\tilde{\nu}_\mu$	$\tilde{\nu}_\tau$	$\tilde{\tau}_1$	$\tilde{\tau}_2$	$\tilde{\chi}_1^0$	$\tilde{\chi}_2^0$	$\tilde{\chi}_1^\pm$
1a	186	185	133	206	96	177	176
1b	328	317	196	344	160	299	299
2	1454	1448	1439	1450	80	135	104
3	276	275	171	289	161	297	297
4	441	389	268	415	119	218	218
5	245	242	181	258	120	226	226

While the small- λ limit simplifies the decay analysis, it also leads to a suppression of the production cross section, which is proportional to λ_{1j1}^2 . We, therefore, focus on the intermediate case, namely⁴ $\lambda_{1j1} \lesssim 0.03$, which while somewhat smaller than the gauge couplings, still allows the sneutrino and LSP to decay almost at the interaction point. With this assumption, the principal decay modes of the sneutrino(s) are those listed in Table II.

The decay modes marked with a λ in Table II occur when the sneutrino decays purely through the R -parity-violating coupling λ_{1j1} . In the remaining modes, the sneutrino decays through R -parity-conserving (gauge) couplings, with an LSP at the final stage of the cascades. The LSP then undergoes a three-body decay through the same λ_{1j1} coupling, with exchange of virtual sleptons. The final states are described without specific leptonic charges, partly because it may be operationally difficult to tag lepton charges, and more importantly, because the Majorana nature of the neutralino enables it to decay to either charge of each leptonic flavor. (This also means that the probability gets multiplied by a factor of 2 for each neutralino when the CP -conjugated process is also considered.) Cascade decays of higher gaugino states to the LSP through a third (intermediate) gaugino state are discounted as the branching ratios are relatively small. Final-state W and Z bosons, will, of course, decay into all possible fermion pairs, according to the branching ratios, increasing the number of possible combinations. Since we are interested only in *hadronically quiet* signals, we do not consider their (dominant) decays to quarks, but focus on the leptonic decays only⁵. Even with this simplification, we still have a large number of possible final states which can appear together with an associated (hard) photon. These are listed in Table III, with the cross sections for the five Snowmass points which are kinematically accessible. The table has been constructed assuming $\lambda_{1j1} = 0.03$ as explained

⁴This value is also consistent with the bounds expected from fermion pair production at a linear collider [15].

⁵In this work, we have not considered final states with jets, not because they are not important for the detection of sneutrinos, but simply because the leptonic final states are cleaner and easier to analyze. It also means that we can use a parton-level Monte Carlo event generator without much error.

TABLE II. Principal decay modes of the sneutrinos $\tilde{\nu}_\mu$ and $\tilde{\nu}_\tau$, including R -parity-violating decays, at five of the six Snowmass 2001 points. We exclude point 2 because it predicts that $\tilde{\nu}$ production would be kinematically disallowed at a 500 GeV or even a 1 TeV collider.

	λ_{121}	λ_{131}	
1a	$\tilde{\nu}_\mu \xrightarrow{\lambda} e^- + e^+$	$\tilde{\nu}_\tau \xrightarrow{\lambda} e^- + e^+$	
	$\rightarrow \nu_\mu + \tilde{\chi}_{1,2}^0$	$\rightarrow \nu_\tau + \tilde{\chi}_{1,2}^0$	
	$\rightarrow \mu^- + \tilde{\chi}_1^+$	$\rightarrow \tau^- + \tilde{\chi}_1^+$	
	$\tilde{\chi}_{1,2}^0 \xrightarrow{\lambda} e^- + e^+ + \bar{\nu}_\mu$	$\tilde{\chi}_{1,2}^0 \xrightarrow{\lambda} e^- + e^+ + \bar{\nu}_\tau$	
	$\xrightarrow{\lambda} e^- + \mu^+ + \bar{\nu}_e$	$\xrightarrow{\lambda} e^- + \tau^+ + \bar{\nu}_e$	
	$\tilde{\chi}_2^0 \rightarrow \tau^- + \tilde{\tau}^+$	$\tilde{\chi}_2^0 \rightarrow \tau^- + \tilde{\tau}^+$	
	$\tilde{\chi}_1^+ \rightarrow \tilde{\tau}^+ + \nu_\tau$	$\tilde{\chi}_1^+ \rightarrow \tilde{\tau}^+ + \nu_\tau$	
	$\tilde{\tau}^+ \rightarrow \tilde{\chi}_1^0 + \tau^+$	$\tilde{\tau}^+ \rightarrow \tilde{\chi}_1^0 + \tau^+$	
	1b	$\tilde{\nu}_\mu \xrightarrow{\lambda} e^- + e^+$	$\tilde{\nu}_\tau \xrightarrow{\lambda} e^- + e^+$
		$\rightarrow \nu_\mu + \tilde{\chi}_{1,2}^0$	$\rightarrow \nu_\tau + \tilde{\chi}_{1,2}^0$
$\rightarrow \mu^- + \tilde{\chi}_1^+$		$\rightarrow \tau^- + \tilde{\chi}_1^+$	
$\rightarrow \tilde{\tau}^- + W^+$		$\rightarrow \tilde{\tau}^- + W^+$	
$\tilde{\chi}_{1,2}^0 \xrightarrow{\lambda} e^- + e^+ + \bar{\nu}_\mu$		$\tilde{\chi}_{1,2}^0 \xrightarrow{\lambda} e^- + e^+ + \bar{\nu}_\tau$	
$\xrightarrow{\lambda} e^- + \mu^+ + \bar{\nu}_e$		$\xrightarrow{\lambda} e^- + \tau^+ + \bar{\nu}_e$	
$\tilde{\chi}_2^0 \rightarrow \tau^- + \tilde{\tau}^+$		$\tilde{\chi}_2^0 \rightarrow \tau^- + \tilde{\tau}^+$	
$\tilde{\chi}_1^+ \rightarrow \tilde{\tau}^+ + \nu_\tau$		$\tilde{\chi}_1^+ \rightarrow \tilde{\tau}^+ + \nu_\tau$	
$\rightarrow \tilde{\chi}_1^0 + W^+$		$\rightarrow \tilde{\chi}_1^0 + W^+$	
$\tilde{\tau}^+ \rightarrow \tilde{\chi}_1^0 + \tau^+$		$\tilde{\tau}^+ \rightarrow \tilde{\chi}_1^0 + \tau^+$	
3	$\tilde{\nu}_\mu \xrightarrow{\lambda} e^- + e^+$	$\tilde{\nu}_\tau \xrightarrow{\lambda} e^- + e^+$	
	$\rightarrow \nu_\mu + \tilde{\chi}_1^0$	$\rightarrow \nu_\tau + \tilde{\chi}_1^0$	
	$\rightarrow \tilde{\tau}^- + W^+$	$\rightarrow \tilde{\tau}^- + W^+$	
	$\tilde{\chi}_1^0 \xrightarrow{\lambda} e^- + e^+ + \bar{\nu}_\mu$	$\tilde{\chi}_1^0 \xrightarrow{\lambda} e^- + e^+ + \bar{\nu}_\tau$	
	$\xrightarrow{\lambda} e^- + \mu^+ + \bar{\nu}_e$	$\xrightarrow{\lambda} e^- + \tau^+ + \bar{\nu}_e$	
	$\tilde{\tau}^+ \rightarrow \tilde{\chi}_1^0 + \tau^+$	$\tilde{\tau}^+ \rightarrow \tilde{\chi}_1^0 + \tau^+$	
4	$\tilde{\nu}_\mu \xrightarrow{\lambda} e^- + e^+$	$\tilde{\nu}_\tau \xrightarrow{\lambda} e^- + e^+$	
	$\rightarrow \nu_\mu + \tilde{\chi}_{1,2}^0$	$\rightarrow \nu_\tau + \tilde{\chi}_{1,2}^0$	
	$\rightarrow \mu^- + \tilde{\chi}_1^+$	$\rightarrow \tau^- + \tilde{\chi}_1^+$	
	$\rightarrow \tilde{\tau}^- + W^+$	$\rightarrow \tilde{\tau}^- + W^+$	
	$\tilde{\chi}_{1,2}^0 \xrightarrow{\lambda} e^- + e^+ + \bar{\nu}_\mu$	$\tilde{\chi}_{1,2}^0 \xrightarrow{\lambda} e^- + e^+ + \bar{\nu}_\tau$	
	$\xrightarrow{\lambda} e^- + \mu^+ + \bar{\nu}_e$	$\xrightarrow{\lambda} e^- + \tau^+ + \bar{\nu}_e$	
	$\tilde{\chi}_2^0 \rightarrow \tilde{\chi}_1^0 + Z$	$\tilde{\chi}_2^0 \rightarrow \tilde{\chi}_1^0 + Z$	
	$\tilde{\chi}_1^+ \rightarrow \tilde{\chi}_1^0 + W^+$	$\tilde{\chi}_1^+ \rightarrow \tilde{\chi}_1^0 + W^+$	
	$\tilde{\tau}^+ \rightarrow \tilde{\chi}_{1,2}^0 + \tau^+$	$\tilde{\tau}^+ \rightarrow \tilde{\chi}_{1,2}^0 + \tau^+$	
	$\tilde{\tau}^+ \rightarrow \tilde{\chi}_1^+ + \bar{\nu}^+$	$\tilde{\tau}^+ \rightarrow \tilde{\chi}_1^+ + \bar{\nu}^+$	
5	$\tilde{\nu}_\mu \xrightarrow{\lambda} e^- + e^+$	$\tilde{\nu}_\tau \xrightarrow{\lambda} e^- + e^+$	
	$\rightarrow \nu_\mu + \tilde{\chi}_{1,2}^0$	$\rightarrow \nu_\tau + \tilde{\chi}_{1,2}^0$	
	$\rightarrow \mu^- + \tilde{\chi}_1^+$	$\rightarrow \tau^- + \tilde{\chi}_1^+$	
	$\rightarrow \tilde{\tau}^- + W^+$	$\rightarrow \tilde{\tau}^- + W^+$	
	$\tilde{\chi}_{1,2}^0 \xrightarrow{\lambda} e^- + e^+ + \bar{\nu}_\mu$	$\tilde{\chi}_{1,2}^0 \xrightarrow{\lambda} e^- + e^+ + \bar{\nu}_\tau$	
	$\xrightarrow{\lambda} e^- + \mu^+ + \bar{\nu}_e$	$\xrightarrow{\lambda} e^- + \tau^+ + \bar{\nu}_e$	
	$\tilde{\chi}_2^0 \rightarrow \tau^- + \tilde{\tau}^+$	$\tilde{\chi}_2^0 \rightarrow \tau^- + \tilde{\tau}^+$	
	$\tilde{\chi}_1^+ \rightarrow \tilde{\tau}^+ + \nu_\tau$	$\tilde{\chi}_1^+ \rightarrow \tilde{\tau}^+ + \nu_\tau$	
	$\rightarrow \tilde{\chi}_1^0 + W^+$	$\rightarrow \tilde{\chi}_1^0 + W^+$	
	$\tilde{\tau}^+ \rightarrow \tilde{\chi}_1^0 + \tau^+$	$\tilde{\tau}^+ \rightarrow \tilde{\chi}_1^0 + \tau^+$	

above. We have convoluted the cross sections in Table II with detection efficiencies $\eta_e \simeq \eta_\mu \simeq 90\%$ and $\eta_\tau \simeq 80\%$, which are consistent with the known LEP-2 efficiency factors and likely to be bettered at the NLC.

TABLE III. Number of events for luminosity $\mathcal{L} = 100 \text{ fb}^{-1}$ for different final states arising from sneutrino decay cascades in (A) $e^+ + e^- \rightarrow \gamma + \tilde{\nu}_\mu(\tilde{\nu}_\mu^*)$ and (B) $e^+ + e^- \rightarrow \gamma + \tilde{\nu}_\tau(\tilde{\nu}_\tau^*)$ at a 500 (1000) GeV $e^+ e^-$ linear collider with unpolarized beams. Columns correspond to the Snowmass points (except the kinematically disallowed 2 point). Entries marked with dots (\dots) indicate less than 10 events. Detection efficiencies are (crudely) included in the cross-section figures.

(A)		1a		1b		3		4		5	
λ_{121}	Final state \sqrt{s} (TeV)	0.5	(1.0)	0.5	(1.0)	0.5	(1.0)	0.5	(1.0)	0.5	(1.0)
1	$\gamma + ee$	559	(123)	823	(113)	1058	(183)	469	(21)	580	(111)
2	$\gamma + ee \cancel{E}$	1592	(349)	2256	(308)	2236	(387)	2601	(115)	1667	(320)
3	$\gamma + e\mu \cancel{E}$	1592	(349)	2256	(308)	2236	(387)	2601	(115)	1667	(320)
4	$\gamma + ee\tau\tau \cancel{E}$	33	(\dots)	88	(12)	\dots	(\dots)	\dots	(\dots)	42	(\dots)
5	$\gamma + e\mu\tau\tau \cancel{E}$	33	(\dots)	88	(12)	\dots	(\dots)	\dots	(\dots)	42	(\dots)
6	$\gamma + eee\mu \cancel{E}$	\dots	(\dots)	\dots	(\dots)	\dots	(\dots)	658	(2.9)	\dots	(\dots)
7	$\gamma + ee\mu\mu \cancel{E}$	\dots	(\dots)	11	(\dots)	\dots	(\dots)	1316	(58)	15	(\dots)
8	$\gamma + ee\mu\tau \cancel{E}$	112	(24)	446	(61)	\dots	(\dots)	585	(26)	194	(37)
9	$\gamma + e\mu\mu\tau \cancel{E}$	112	(24)	446	(61)	\dots	(\dots)	585	(26)	194	(37)
10	$\gamma + e\mu\mu\mu \cancel{E}$	\dots	(\dots)	\dots	(\dots)	\dots	(\dots)	658	(29)	\dots	(\dots)

(B)		1a		1b		3		4		5	
λ_{131}	Final state \sqrt{s} (TeV)	0.5	(1.0)	0.5	(1.0)	0.5	(1.0)	0.5	(1.0)	0.5	(1.0)
1	$\gamma + ee \cancel{E}$	576	(126)	547	(79)	949	(165)	256	(22)	521	(101)
2	$\gamma + ee \cancel{E}$	1618	(355)	1387	(200)	1987	(345)	1157	(100)	1464	(283)
3	$\gamma + e\tau \cancel{E}$	1438	(316)	1233	(178)	1766	(307)	1029	(89)	1301	(251)
4	$\gamma + ee\tau\tau \cancel{E}$	108	(24)	350	(50)	41	(\dots)	527	(46)	155	(30)
5	$\gamma + e\tau\tau\tau \cancel{E}$	96	(21)	217	(31)	18	(\dots)	234	(20)	134	(26)
6	$\gamma + eee\tau \cancel{E}$	\dots	(\dots)	119	(17)	23	(\dots)	297	(26)	\dots	(\dots)
7	$\gamma + ee\mu\tau \cancel{E}$	\dots	(\dots)	119	(17)	23	(\dots)	297	(26)	\dots	(\dots)
8	$\gamma + e\mu\tau\tau \cancel{E}$	\dots	(\dots)	106	(15)	21	(\dots)	264	(23)	\dots	(\dots)

Table III shows that the 18 types of R -parity-violating signals resolve themselves into four classes. These are

- (1) photon plus dielectron;
- (2) photon plus dielectron plus missing energy;
- (3) photon plus dileptons of dissimilar flavor plus missing energy;
- (4) photon plus four leptons plus missing energy.

The first kind arises from the direct R -parity-violating decay of the sneutrino and would have a large SM background from radiative Bhabha scattering. The second and third ones are obviously reproduced by WW production. The last type arises from higher-order effects in the SM and has very little background. Thus each signal requires to be discussed separately and specific cuts and isolation techniques need to be applied in each case. Of course, the trigger will still be a (approximately) monochromatic photon, which results from its recoil against the resonant sneutrino. We now take up the study of these signals in detail.

IV. SIGNAL ISOLATION

In this section we discuss various strategies for identifying the signals that a sneutrino (of muonic or tauonic) flavor has been produced in e^+e^- interactions at a linear collider and has decayed subsequently. The numerical

analysis has been carried out for center-of-mass energy of 500 GeV for both the cases, viz. the associated production of $\tilde{\nu}_\mu$ or of $\tilde{\nu}_\tau$ and their subsequent cascades to the four classes of R -parity-violating signals listed above. We note that the analysis at a 500 GeV linear collider provides sufficient physics insight into isolating the R -parity-violating signal, and renders an analysis of a 1 TeV machine, at this stage, redundant. Similarly, we have mostly analyzed the luminosity option $\mathcal{L} = 100 \text{ fb}^{-1}$, since that provides conservative estimates of statistical fluctuations in the SM background.

This section has been broken up into four subsections for the four classes of signals listed above and we have presented differential cross sections for the parameters which show the most significant deviations from the standard model background. The latter involves the calculation of many diagrams, and has been generated using the MadGraph package [27] and the Madevent [28] Monte Carlo generator.

A. The $e^+e^- \gamma$ final state

This final state arises from the direct R -parity violating decay of the sneutrino into an e^+e^- pair, with, of course an associated photon from the initial state. The branching ratio of the sneutrino to this mode is quite significant for

$\lambda_{1j1} \sim 0.03$ and hence the signal has a reasonable cross section. To detect this final state, we impose a set of acceptance sets, namely, that each of the particles must not be too close to the beam pipe,

$$|\eta(e^\pm)|, |\eta(\gamma)| < 2.0 \quad (9)$$

and that they should carry sufficient transverse momenta

$$p_T(e^\pm) > 10 \text{ GeV} \quad \text{and} \quad p_T(\gamma) > 20 \text{ GeV}. \quad (10)$$

In addition, each pair of the final-state particles should be well separated:

$$\delta R > 0.2, \quad (11)$$

where $(\delta R)^2 \equiv (\Delta\phi)^2 + (\Delta\eta)^2$ with $\Delta\eta$ and $\Delta\phi$ respectively denoting the separation in rapidity and azimuthal angle. Even with such cuts, the SM background, originating from radiative Bhabha scattering, far overwhelms the signal, in fact almost by a factor of 200. It is thus imperative to identify phase space variables that would be preferentially sensitive to scalar production thereby accentuating the signal to noise ratio. An obvious such variable is the energy E_γ of the recoil photon, which would be monochromatic in the case of the signal and a continuum for the background. However, before we consider E_γ , it is more useful to consider the difference between the fermion rapidities, namely

$$\Delta\eta_{ee} = \eta_{e^+} - \eta_{e^-}. \quad (12)$$

While the signal peaks at zero and is symmetric about it, the SM background is highly skewed towards positive $\Delta\eta_{ee}$ on account of the strong t -channel photon contribution to (radiative) Bhabha scattering (see Fig. 3). Thus, if charge measurement of the electron and positron is straightforward and very efficient, requiring $\Delta\eta < 0$ would reduce the signal by only a factor of 2 while eliminating a very large part of the background. However, even if charge identification is not possible (or efficient), we could still consider $|\Delta\eta_{ee}|$, rather than $\Delta\eta_{ee}$ itself. Clearly, cutting off higher values of $|\Delta\eta_{ee}|$ can reduce the background considerably without significantly hurting the signal. A detailed evaluation shows that

$$|\Delta\eta_{ee}| \leq 1.7 \quad (13)$$

is the most suitable cut, i.e. the one which produces the largest significance $N_{\text{signal}}/\sqrt{N_{\text{SM}}}$, where $N = \sigma\mathcal{L}$. With this cut, the signal is reduced only by around 25% (with slight variations for different Snowmass points), while the background is reduced by a factor larger than 4. We have, therefore, implemented this cut in our subsequent numerical analysis of the $\gamma e^+ e^-$ signal.

We may now consider distributions in (a) E_γ , which is our trigger, (b) the invariant mass M_{ee} of the $e^+ e^-$ pair in the final state, which should peak at the resonant mass, and (c) the opening angle θ_{ee} between the $e^+ e^-$ pair. While E_γ and M_{ee} are essentially the same observable in this case,

we nonetheless include it as a counterpoint to the other cases to be discussed below.

In Fig. 4 we show the signal distributions for the case $\lambda_{121} = 0.03$ in the above variables with binnings which are more-or-less consistent with the resolution(s) expected at a high-energy $e^+ e^-$ collider, like, for example, Tesla. These are represented by colored histograms for the Snowmass points 1a, 1b, 3, 4, and 5. Rather than showing the large SM backgrounds, we have given the statistical (Gaussian) fluctuations at 1, 3, and 5 standard deviations. It is immediately apparent that the photon spectrum will show clear peaks corresponding to recoil against a sneutrino. This feature, expectably, repeats itself in the invariant mass distribution.

The opening angle between the $e^+ e^-$ pair also shows peaks tailing off towards large angles, but with a clear lower cutoff depending on the sneutrino mass. It is clear that the signal is somewhat less prominent, but still discernible, when we consider this variable. This graph has been drawn assuming a luminosity $\mathcal{L} = 1000 \text{ fb}^{-1}$, unlike the previous ones, which are for $\mathcal{L} = 100 \text{ fb}^{-1}$.

Finally, we should note that, for this particular final state, the signal is extremely sensitive to the value of λ_{121} . This is because both the sneutrino production cross section and the sneutrino branching ratio to an $e^+ e^-$ pair are proportional to λ_{121}^2 . This quartic dependence ensures that even a moderately lower value such as $\lambda_{121} = 0.01$ will ensure that the signal is hardly discernible over the SM background even with the high luminosity option $\mathcal{L} = 10^3 \text{ fb}^{-1}$. The same features repeat themselves for the λ_{131} coupling. We therefore turn to the other possible final states, which are related to more robust decay modes of the sneutrino resonance.

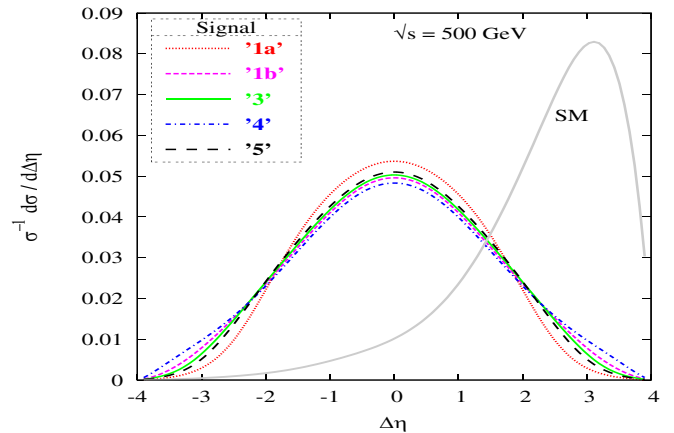


FIG. 3 (color online). The normalized distribution in the difference of electron and production rapidities for the $e^+ e^- \gamma$ final states at a 500 GeV linear collider, and for the different Snowmass points. Also shown in gray is the SM background. The cuts of Eqs. (9)–(11) have been imposed.

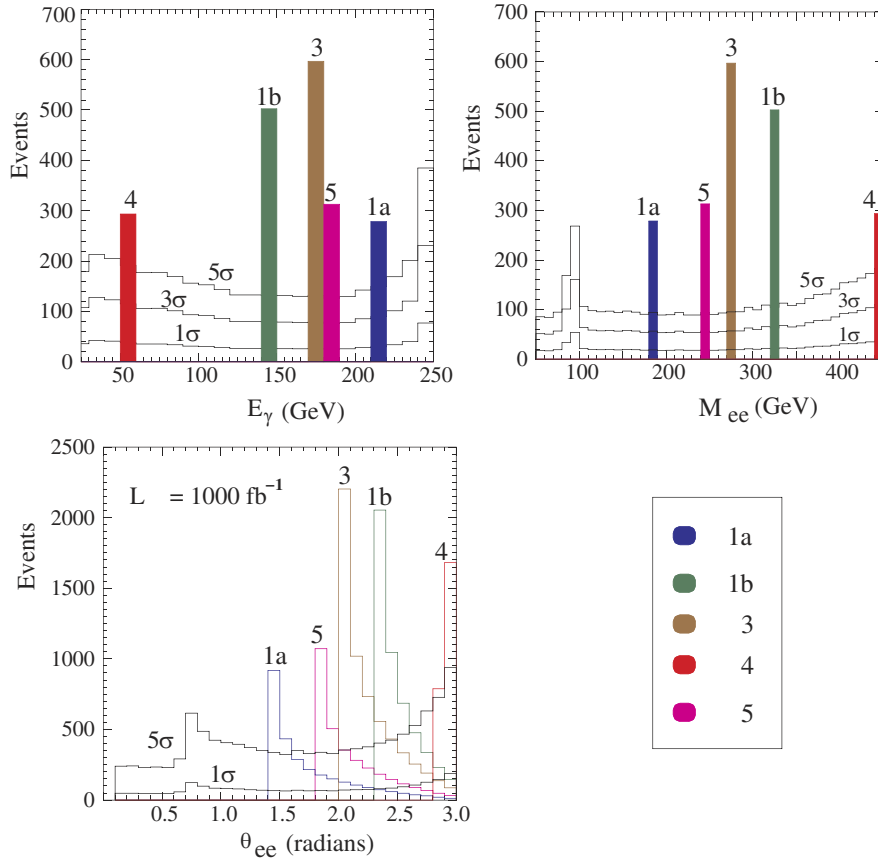


FIG. 4 (color online). Illustrating kinematic distributions for the $e^+e^-\gamma$ final states at a 500 GeV linear collider. Snowmass points are indicated with shading (colors) and black lines correspond to statistical fluctuations in the SM background. The cuts of Eqs. (9)–(13) have been imposed. The first two graphs correspond to luminosity $L = 100 \text{ fb}^{-1}$.

B. $e^+e^-\gamma\cancel{E}_T$ final states

This final state differs from the last in having a substantial amount of missing energy in addition to a trigger photon and an e^+e^- pair in the final state. A glance at Table III will establish the fact that this channel corresponds to large branching ratios both for the λ_{121} and λ_{131} cases. It arises (see Table II) from the R -parity-conserving decay of a sneutrino to a same-flavor lepton and a neutralino, followed by three-body decay of the neutralino through the R -parity violating coupling, with the missing energy component coming from neutrinos in the final state. Since the decay of the sneutrino to neutralinos is governed by gauge couplings, this channel is suppressed only quadratically by lower values of λ_{1j1} —and is hence considerably more robust than the channel considered in the previous subsection. Moreover, the SM background, which comes from higher-order processes than radiative Bhabha scattering, is only at the level of about 36 events for $\mathcal{L} = 10 \text{ fb}^{-1}$, which is considerably below the signal, which is in excess of a hundred events, as shown in Table III. Thus, one can expect an excess in the total cross section over fluctuations in the background even for λ_{1j1} as low as 0.01. For the differential cross sections, the deviations are even

more striking and hence much lower values of the λ_{1j1} coupling can be probed.

Before proceeding further, it is necessary to delineate the kinematic requirements that we seek to impose. As for the leptons and the photon, we choose the cuts to be the same as before, namely, those listed in Eqs. (9)–(11). In addition, we demand that the missing transverse momentum be sufficiently large, viz.

$$\cancel{p}_T > 20 \text{ GeV} \quad (14)$$

for it to be considered a genuine physics effect. Since the SM backgrounds have a different source from the last case, it is not meaningful to implement a cut on $|\Delta\eta_{ee}|$.

The kinematic variables of interest for this channel are similar, but somewhat different from the last case. As before, the recoil photon spectrum (E_γ) should show a peak corresponding to the resonance, and indeed it does, as a glance at Fig. 5 will show. Since we have chosen $\lambda_{121} = 0.03$ for this graph, the peaks are tall and sharp and cannot be missed by any means. In fact, these are roughly 2 orders of magnitude above the 5σ background fluctuation, which means that we will get observable effects even if λ_{121} is an order of magnitude smaller, say $\lambda_{121} \approx 0.003$.

The other variables plotted in Fig. 5 are as follows. The e^+e^- invariant mass is no longer peaked at the sneutrino mass since one of the e^+ and e^- arises from three-body decays of the neutralino. However, there is still a substantial deviation from the background fluctuations. In fact, the second graph in Fig. 5 shows that for low values of λ_{121} , the signal can be considerably enhanced by imposing a kinematic cut $M_{ee} < 250$ GeV. The third box shows the distribution in photon transverse momentum, which, for smaller λ_{121} will show modest deviations at the right end. The last box shows the e^+e^- opening angle θ_{ee} , which likewise shows deviations at the lower end. It is worth mentioning that there is no significant deviation in the shape of the missing energy and momentum curves, though, of course, there will be an overall excess if λ_{121} is large enough.

We have not exhibited the curves for a λ_{131} coupling because they reproduce the same qualitative features, though the actual numerics has slight differences.

C. $e\mu\gamma\cancel{E}_T$ and $e\tau\gamma\cancel{E}_T$ final states

The presence of an R -parity-violating coupling also ensures that there will be significant numbers of sneutrinos which decay through channels with a final-state μ^\pm or a

final-state τ^\pm in addition to a photon and an electron. Such decay modes will also have substantial missing energy from escaping neutrinos. Since the neutrino flavors cannot be tagged, there will also be a substantial background from SM processes with W^+W^- pairs. If the R -parity-violating coupling is λ_{121} we can expect $e\mu$ combinations, while if the coupling is λ_{131} we can expect $e\tau$ combinations. However, the cross sections are not identical, since the cascade decays are not the same. This is due to the presence of low-lying $\tilde{\tau}$ states for the Snowmass points under consideration.

The analysis of these final states follows that of the $\gamma e^+e^- \cancel{E}_T$ state quite closely. We impose precisely the same kinematic cuts on the μ^\pm or τ^\pm as was imposed on the electron and keep other cuts also the same. As in that case, the signal cross sections for $\lambda_{1j1} = 0.03$ are quite large and, in fact, quite a few times larger than the background, which, for $\mathcal{L} = 10 \text{ fb}^{-1}$ is at the level of about 22 events for both $e\mu\gamma\cancel{E}_T$ and $e\tau\gamma\cancel{E}_T$ final states. Once again, the signal is expected to fall as λ_{1j1} decreases, in which case it would be necessary to look at the differential cross sections. These, in turn, will resemble those of Fig. 5 closely, because the actual kinematics is very similar, all leptons appearing massless at the energies under consid-

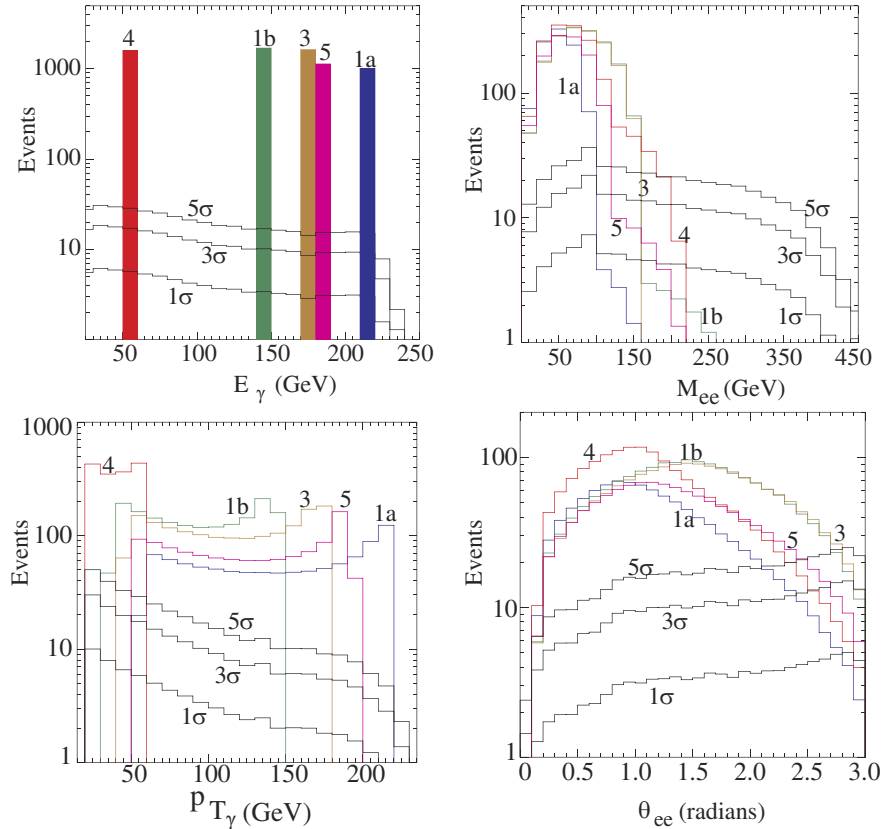


FIG. 5 (color online). Illustrating the distributions in the excess in events over SM predictions for the $e^+e^- \gamma \cancel{E}_T$ final states at a 500 GeV linear collider. The cuts of Eqs. (9)–(11) and (14) have been imposed. The shading is the same as in Fig. 4. The RPV coupling involved here is 121 and the luminosity is $L = 100 \text{ fb}^{-1}$.

eration. In the interests of brevity, we do not exhibit the actual graphs, but merely note the following points:

- (i) The photon spectrum is, as usual, peaked at values corresponding to the sneutrino mass.
- (ii) The $e\ell$ ($\ell = \mu, \tau$) invariant mass does not show sharp peaks, but shows a kinematic boundary around $M_{e\ell} \simeq \sqrt{s}/2$.
- (iii) The transverse momentum of the photon peaks at high values around 200 GeV. This feature distinguishes it from the background fluctuations, which tend to fall uniformly as $p_{T\gamma}$ increases. The peaking, which is very prominent in the figure shown, would become more modest if λ_{1j1} were decreased.
- (iv) The $e\ell$ opening angle shows modest (for smaller λ_{1j1}) peaking in the first quadrant, which again deviates from the background, which prefers a back-to-back $e\ell$ pair.
- (v) The missing transverse momentum (\cancel{p}_T) distribution is almost identical with that of the background. The most important feature of the $e\mu\gamma\cancel{E}_T$ and $e\tau\gamma\cancel{E}_T$ final states is that if a sneutrino is produced in sufficient numbers then one of the two final states will exhibit an excess over the SM background if the $ee\gamma\cancel{E}_T$ state shows an excess. The other will not, unless, indeed, both the λ_{121} and λ_{131} couplings are present⁶. The existence of both a $ee\gamma\cancel{E}_T$ and a $e\mu\gamma\cancel{E}_T$ signal is a hallmark of a muonic sneutrino $\tilde{\nu}_\mu$, while the existence of both a $ee\gamma\cancel{E}_T$ and a $e\tau\gamma\cancel{E}_T$ signal indicates production of a tau sneutrino $\tilde{\nu}_\tau$. Thus, establishing the existence of the signal is the primary goal of the analysis, and this, of course, is facilitated by considering the kinematic distributions discussed above.

D. Multilepton final states

Ten of the 18 final states listed in Table III consist of a hard photon and four identifiable leptons, of different flavors. The number of events expected in these channels varies very widely, as a glance at Table III will show. Nevertheless, these channels have practically no SM background, as a simple consideration will show. We have already noted that the cross section for producing a photon and two leptons is at the level of about 2 fb. To have two more, we require to radiate a further gauge boson, which then decays leptonically. This leads to suppression by at least the electromagnetic coupling α , i.e. by 2 orders of magnitude, provided, of course, that we assume minimum isolation criteria for every pair of leptons. We thus predict SM backgrounds at the level of 0.01 fb. By contrast, the R -parity-violating signal is at the level of a femtobarn, which

⁶There are strong constraints on the product $\lambda_{121}\lambda_{131}$ from the nonobservation of various decays forbidden in the standard model such as $\tau \rightarrow \mu\gamma$ or $\tau \rightarrow 3e$ [25]. It is, therefore, usual to set one of them to zero. This is also consistent with our declared policy of considering only one dominant coupling.

means that it will stand out very clearly over the background.

The presence of large numbers of leptons in the final state is generally a signal for dileptons or of R -parity-violating couplings, though the actual violation of lepton number cannot be empirically established. This is because the missing energy and momentum component could be due to an unknown number of neutrinos carrying the necessary flavors to keep lepton number conserved. Nevertheless, such explanations have been tried earlier, whenever (seemingly) unexpected numbers of leptons have appeared in the final state. For the present case, in addition to the presence of four leptons (of which one is always an electron), we have a hard associated photon, whose energy will peak at a value indicative of the sneutrino resonance. The combination of such a monoenergetic photon with multilepton final states, and with a cross section at the femtobarn level, would be difficult to explain away by any other hypothesis than the present one.

It is important, however, not to be too upbeat about photon plus four-lepton final states as a signature of R -parity-violating sneutrinos. This is because the cross section for such states depends heavily on the neutralino couplings and hence on the point in the parameter space. For example, Table III shows that, for a λ_{121} coupling, there are no such signals even at the 0.1 fb level for the Snowmass point 3. Absence of such signals, then, is not unexpected, and should not be construed in a negative sense for the model.

In fact, of the above set of signals for sneutrino decay, the most important points to note are (a) the monoenergetic photon, and (b) the presence of one or more of the different final states arising from sneutrino decay, which can be isolated from the background by considering the distributions exhibited in Figs. 4 and 5. Though we may not observe the full set of final states, we should certainly see *something*, which would then clearly point to recoil of the photon against a resonant particle with leptophilic couplings.

V. DISTINGUISHING A SCALAR FROM A VECTOR RESONANCE

As we have demonstrated in the previous section, it should be possible, for a wide range of parameters, to establish a resonance by triggering on a recoil photon of fixed energy and identifying a variety of associated final states with leptons and missing energy. However, it requires some more effort to identify the resonance with a sneutrino of R -parity-violating supersymmetry. The first step in such an exercise would be to determine the spin of the resonance, a task that is best performed by analyzing the angular distributions.

As far as the photon's distribution is concerned, it is primarily driven by its $t(u)$ channel nature and hence is not very sensitive to the spin of the resonance. Similarly, for the γe^+e^- final state, it is not enough to construct just the

angular distribution of the electron/positron in the laboratory frame. For, with the dilepton system recoiling against the photon, the effect of the consequent boost tends to mask the smaller differences due to spin. Thus, the recoil needs to be corrected for, or, in other words, we need to construct the angular distribution in the *rest frame* of the e^+e^- pair, i.e. of the resonance. Denoting the angle between the final-state e^+/e^- and the parent resonance (whose direction is identical with the boost axis, which in turn is opposite to that of the photon) by θ_e , we construct the distribution in $x \equiv \cos\theta_e$. This is exhibited in Fig. 6, where the dashed red (solid blue) histograms illustrate the normalized distribution expected for scalar (vector) particles.

Even a cursory glance at the figure shows that there is a clear difference between the more-or-less flat scalar distribution and the vector distribution which shows a moderate depletion in the transverse direction. In order to see if these would be actually observable, we need to make an estimate of the possible errors in the histogram(s) of Fig. 6. For a cross section $\sigma_S \simeq 60$ fb and a luminosity of 100 fb^{-1} , the error in the normalized cross section comes out to be of the order of 0.01, which is clearly much smaller than the actual difference between the two histograms. It follows that one should be able to make a clear distinction between a scalar and a vector resonance in γe^+e^- final states.

The other final states considered in the previous section, which contain a substantial missing energy component, are not amenable to the reconstruction discussed above. Hence, for a small R -parity-violating coupling, e.g. $\lambda_{1j1} \sim 0.01$, it may be difficult to identify the scalar nature of the resonance with any certainty. Of course, we always have the option of collecting higher luminosity, in which case there will be a significant number of γe^+e^- final states.

A different method presents itself in the context of beam polarization. While we have, until now, considered only unpolarized beams, a high degree of beam polarization is a realistic possibility at a high-energy linear e^+e^- collider, and could be of considerable help in enhancing the signal *vis-à-vis* background for many of the distributions shown in the text. Furthermore, note that while the process $e^+e^- \rightarrow \gamma V$, with V denoting a generic spin-one particle is enhanced if the electron and the positron have opposite helicities, the case of the (pseudo-)scalar S prefers the helicities to be the same. In general, if η_1 and η_2 be the helicity states of the initial e^+e^- pair, then we have

$$\begin{aligned} \sigma(e^+e^- \rightarrow \gamma S) &\propto (1 + \eta_1\eta_2)(|S|^2 + |\mathcal{P}|^2) \\ &\quad + 2(\eta_1 + \eta_2)\text{Re}(S\mathcal{P}^*) \quad \text{for } (S + \mathcal{P}\gamma_5), \\ \sigma(e^+e^- \rightarrow \gamma V) &\propto (1 - \eta_1\eta_2)(v^2 + a^2) \\ &\quad - 2va(\eta_1 - \eta_2) \quad \text{for } \gamma_\mu(v + a\gamma_5). \end{aligned} \quad (15)$$

It follows that (a) correct beam polarization can enhance the signal by a factor as large as 4 (assuming 100% beam polarization), while the opposite polarization can com-

pletely kill the signal, and (b) the beam polarization which is good for detecting a scalar resonance is bad for detecting a vector resonance, and vice versa. In fact, this is another way to distinguish between scalar and vector resonances, if we can choose the beam polarizations at will. Even without maximal polarization, a study of the polarization dependence can obviously shed much light on this issue. We, however, desist from discussing this any further as we feel that it calls for a separate study in its own right.

One final question remains. Assuming that we have seen a scalar dilepton, how do we know if it is a sneutrino of R -parity-violating supersymmetry, or a dilepton of some other model (e.g. a composite dilepton)? The answer lies in the observation, or otherwise, of photon plus four-lepton final states, which, as we have seen, arise principally from the decay of heavier gaugino states. The mere presence of such states is an indication that the underlying model is supersymmetry. A detailed discussion of these is beyond the scope of this work and, indeed, premature at this stage. We also sound a note of caution that such four-lepton final states may not always be observable, as pointed out in the last section.

VI. SUMMARY AND CONCLUSIONS

An e^+e^- collider, with its small backgrounds, could be an ideal machine to discover supersymmetry without R parity, especially the lepton-number-violating variety. The presence of $LL\bar{E}$ operators allows us to have sneutrino exchanges, which increases the total four-fermion cross sections. When the coupling is too small for such effects to show up, it is still possible, if the sneutrino is light enough, to excite sneutrino ($\tilde{\nu}_\mu$ or $\tilde{\nu}_\tau$) resonances in e^+e^- collisions. However, this would happen only if the machine energy is tuned to the resonance, which is unlikely. We, therefore, suggest a study of sneutrino production in association with a photon radiated from the initial state, in which case the necessary spread in energy is obtained and large resonant cross sections result, even with the $\mathcal{O}(\alpha)$ suppression. When we take into account the fact that the sneutrino can decay through its R -parity-conserving (gauge) couplings as well as its R -parity-violating λ_{1j1} coupling, four classes of final states result. All of these are characterized by a monoenergetic photon, which corresponds to recoil against a resonant sneutrino.

The first of these, viz. $ee\gamma$, is present only if the λ_{1j1} is large enough and is perhaps the best signal for sneutrino production. It is characterized, apart from a monoenergetic photon, by strong peaks in the e^+e^- invariant mass and opening angle and modest excesses in the rapidity difference between e^+ and e^- . In this case, we can also reconstruct the final-state e^\pm angular distribution in the e^+e^- center-of-mass frame and thereby find a clear distinction between a scalar and a vector resonance with identical decay modes. If found, this would serve to clinch the issue of whether the resonance seen is indeed a sneutrino and

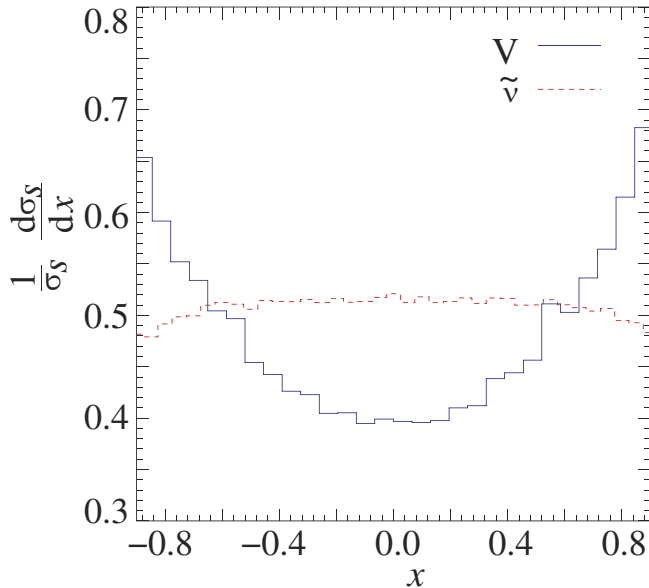


FIG. 6 (color online). Illustrating the distribution in normalized differential cross section of the signal (excess over SM) with respect to $x = \cos\theta_e$. The dashed red (solid blue) curve shows the expectation for a scalar (vector) resonance.

not, for example, a vector dilepton. Next, we have $e\ell\gamma\not{E}_T$ states, where $\ell = e, \mu, \tau$, of which one of the combinations $\ell = e, \mu$ or $\ell = e, \tau$ is expected to show excesses over the SM background, while the third will not. In both cases, we predict, apart from a peak in the photon spectrum, a softer $e\ell$ invariant mass distribution than the SM and modest

excesses in the photon distribution at high transverse momentum and in low values of the e^+e^- opening angle. Finally, we have a monoenergetic photon accompanied by four leptons, of various flavors, in different combinations. These have very little SM background and, if the cross sections are large enough, would be practically (if not quite) smoking-gun signals of R -parity-violating supersymmetry.

In this work, then, we have studied sneutrino production in association with a recoil photon. We have shown that the spread in energies induced by the photon radiation causes a “return to the sneutrino peak” and enables a high-energy e^+e^- collider to act, in a sense, as a sneutrino factory, if the supersymmetric model does not conserve R parity. Not only will this extend the search range in the λ_{1j1} parameter far beyond what a naive study of excesses in dilepton final states could achieve, but different final states will serve to establish the case for a sneutrino resonance and to pin down the R -parity-violating coupling responsible for the process(es). We have shown sample studies at the Snowmass points in the R -parity-conserving sector of the parameter space. Though far from exhaustive, these serve to illustrate our point, and are expected to be a useful guide to experimental physicists searching for supersymmetry when the high-energy e^+e^- collider is finally built and commences operation.

ACKNOWLEDGMENTS

D. C. thanks the Department of Science and Technology, India for financial support.

-
- [1] P. Fayet, Phys. Lett. B **69**, 489 (1977).
 [2] G. R. Farrar and P. Fayet, Phys. Lett. B **76**, 575 (1978).
 [3] L. E. Ibanez and G. G. Ross, Nucl. Phys. **B368**, 3 (1992).
 [4] H. Dreiner and G. G. Ross, Nucl. Phys. **B410**, 188 (1993).
 [5] T. Affolder *et al.*, Phys. Rev. Lett. **89**, 041802 (2002); B. Abbott *et al.* (D0 Collaboration), Phys. Rev. Lett. **83**, 4476 (1999); F. Abe *et al.* (CDF Collaboration), Phys. Rev. Lett. **83**, 2133 (1999); D. Choudhury and S. Raychaudhuri, Phys. Rev. D **56**, 1778 (1997).
 [6] C. Adloff *et al.* (H1 Collaboration), Z. Phys. C **74**, 191 (1997); J. Breitweg *et al.* (ZEUS Collaboration), Z. Phys. C **74**, 207 (1997).
 [7] V. Barger, G. F. Giudice, and T. Han, Phys. Rev. D **40**, 2987 (1989).
 [8] G. Bhattacharyya and D. Choudhury, Mod. Phys. Lett. A **10**, 1699 (1995).
 [9] Some studies are R. M. Godbole, P. Roy, and X. Tata, Nucl. Phys. **B401**, 67 (1993); A. S. Joshipura, V. Ravindran, and S. K. Vempati, Phys. Lett. B **451**, 98 (1999); M. Drees, S. Pakvasa, X. Tata, and T. ter Veldhuis, Phys. Rev. D **57**, R5335 (1998); E. J. Chun and J. S. Lee, Phys. Rev. D **60**, 075006 (1999); A. Abada and M. Losada, Nucl. Phys. **B585**, 45 (2000); A. S. Joshipura, R. Vaidya, and S. K. Vempati, Phys. Rev. D **65**, 053018 (2002); F. Borzumati and J. S. Lee, Phys. Rev. D **66**, 115012 (2002).
 [10] H. Klapdor-Kleingrothaus *et al.*, Prog. Part. Nucl. Phys. **32**, 261 (1994); J. W. F. Valle, hep-ph/9509306; G. Bhattacharyya, H. Klapdor-Kleingrothaus, and H. Pas, Phys. Lett. B **463**, 77 (1999).
 [11] For a summary of these limits, see, for example, G. Bhattacharyya, in *Beyond the Desert: Proceedings of the Fourth Tegernsee International Conference on Particle Physics Beyond the Standard Model, Castle Ringberg, Tegernsee, Germany, 1997* (Springer, New York, 2004); B. C. Allanach, A. Dedes, and H. K. Dreiner, Phys. Rev. D **60**, 075014 (1999); M. Chemtob, Prog. Part. Nucl. Phys. **54**, 71 (2005); R. Barbier *et al.*, Phys. Rep. (to be published).
 [12] E. A. Baltz and P. Gondolo, Phys. Rev. D **57**, 2969 (1998);

- H. Dreiner, P. Richardson, and M.H. Seymour, *J. High Energy Phys.* **04** (2000) 008; F. Borzumati, R.M. Godbole, J.L. Kneur, and F. Takayama, *J. High Energy Phys.* **07** (2002) 037.
- [13] S. Dawson, *Nucl. Phys.* **B261**, 297 (1985).
- [14] F. Borzumati, J.L. Kneur, and N. Polonsky, *Phys. Rev. D* **60**, 115011 (1999); G. Moreau, E. Perez, and G. Polesello, *Nucl. Phys.* **B604**, 3 (2001); H. Dreiner, P. Richardson, and M.H. Seymour, *Phys. Rev. D* **63**, 055008 (2001); D. Choudhury, S. Majhi, and V. Ravindran, *Nucl. Phys.* **B660**, 343 (2003).
- [15] D. Choudhury and S. Raychaudhuri, hep-ph/9807373.
- [16] D. Choudhury and S. Raychaudhuri, *Phys. Lett. B* **401**, 54 (1997); G. Altarelli *et al.*, *Nucl. Phys.* **B506**, 3 (1997); H. Dreiner and P. Morawitz, *Nucl. Phys.* **B503**, 55 (1997); J. Kalinowski *et al.*, *Z. Phys. C* **74**, 595 (1997); T. Kon and T. Kobayashi, *Phys. Lett. B* **409**, 265 (1997); G. Altarelli, G.F. Giudice, and M.L. Mangano, *Nucl. Phys.* **B506**, 29 (1997); J. Ellis, S. Lola, and K. Sridhar, *Phys. Lett. B* **408**, 252 (1997); M. Carena, D. Choudhury, S. Raychaudhuri, and C.E.M. Wagner, *Phys. Lett. B* **414**, 92 (1997).
- [17] D.K. Ghosh, S. Raychaudhuri, and K. Sridhar, *Phys. Lett. B* **396**, 177 (1997).
- [18] T. Han and M.B. Magro, *Phys. Lett. B* **476**, 79 (2000); K. J. Abraham, K. Whisnant, J.M. Yang, and B.L. Young, *Phys. Rev. D* **63**, 034011 (2001).
- [19] G. Bhattacharyya, D. Choudhury, and K. Sridhar, *Phys. Lett. B* **349**, 118 (1995); D. Choudhury, R.M. Godbole, and G. Polesello, *J. High Energy Phys.* **08** (2002) 004.
- [20] J. Kalinowski, R. Rückl, H. Spiesberger, and P.M. Zerwas, *Phys. Lett. B* **414**, 297 (1997).
- [21] J.L. Hewett and T.G. Rizzo, *Phys. Rev. D* **56**, 5709 (1997).
- [22] E.L. Berger, B.W. Harris, and Z. Sullivan, *Phys. Rev. D* **63**, 115001 (2001); K. Hikasa, J.M. Yang, and B. Young, *Phys. Rev. D* **60**, 114041 (1999); D. Choudhury, *Phys. Lett. B* **346**, 291 (1995); A. Datta, *Phys. Rev. D* **65**, 054019 (2002).
- [23] M. Carena, D. Choudhury, S. Lola, and C. Quigg, *Phys. Rev. D* **58**, 095003 (1998); M. Carena, D. Choudhury, C. Quigg, and S. Raychaudhuri, *Phys. Rev. D* **62**, 095010 (2000).
- [24] J. Erler, J.L. Feng, and N. Polonsky, *Phys. Rev. Lett.* **78**, 3063 (1997); J.L. Feng, J.F. Gunion, and T. Han, *Phys. Rev. D* **58**, 071701 (1998).
- [25] K. Agashe and M. Graesser, *Phys. Rev. D* **54**, 4445 (1996); D. Choudhury and P. Roy, *Phys. Lett. B* **378**, 153 (1996); F. Vissani and A.Yu. Smirnov, *Phys. Lett. B* **380**, 317 (1996).
- [26] S.K. Rai and S. Raychaudhuri, *J. High Energy Phys.* **10** (2003) 020.
- [27] T. Stelzer and W.F. Long, *Comput. Phys. Commun.* **81J**, 357 (1994).
- [28] F. Maltoni and T. Stelzer, *J. High Energy Phys.* **02** (2003) 027.